Journal of Inflammation Research

Dovepress
open access to scientific and medical research

Open Access Full Text Article

ORIGINAL RESEARCH

Suppression of P2X7R by Local Treatment Alleviates Acute Gouty Inflammation

Yang Zhao[1–3], Zhiyuan Li[2], Ying Chen[3–5], Yushuang Li[3–5], Jie Lu[2–5]

[1]Department of Orthodontics, the Affiliated Hospital of Qingdao University, Qingdao, People's Republic of China; [2]Medical Research Center, the Affiliated Hospital of Qingdao University, Qingdao, People's Republic of China; [3]Shandong Provincial Key Laboratory of Metabolic Diseases and Qingdao Key Laboratory of Gout, the Affiliated Hospital of Qingdao University, Qingdao, People's Republic of China; [4]Shandong Provincial Clinical Research Center for Immune Diseases and Gout, the Affiliated Hospital of Qingdao University, Qingdao, People's Republic of China; [5]Department of Endocrinology and Metabolism, the Affiliated Hospital of Qingdao University, Qingdao, People's Republic of China

Correspondence: Jie Lu, Shandong Provincial Key Laboratory of Metabolic Diseases and Qingdao Key Laboratory of Gout, the Affiliated Hospital of Qingdao University, 16 Jiangsu Road, Qingdao, Shandong, 266003, People's Republic of China, Tel +86 17853297395, Fax +86 0532-82912019, Email 13127006046@163.com

Objective: Gout is the most common inflammatory arthritis associated with interleukin-1β (IL-1β) accumulation during exacerbation. In this study, we aimed to clarify whether potassium channel antagonists attenuate local inflammation in mice with monosodium urate (MSU)-induced gout.

Methods: We cultured human macrophage THP-1 cells and evaluated the molecular levels of both IL-1β and potassium channels stimulated with MSU and/or potassium channel antagonists. Acute gout models were generated in IL-1β luciferase transgenic male mice using synovium-like subcutaneous air pouches with MSU injection. Their luciferase activities were monitored following potassium channel blocker treatment using the IVIS Spectrum CT imaging system. The lavages and tissues were extracted from their air pouches, followed by cell counting and pathological analysis.

Results: MSU stimulation increased the gene expression levels of *pro-IL-1β, P2x7r* and *Kv1.3*, whereas the expression of *Kcnq1* was decreased in phorbol 12-myristate 13-acetate-induced THP-1 cells. Both high and low concentrations of the P2x7 receptor inhibitor adenosine 5′-triphosphate (ATP) derivative periodate oxidized ATP (oATP) decreased the production of IL-1β in the supernatant of THP-1 cells. The sixth hour was the peak time of IL-1β luciferase activity after MSU intervention in vivo. oATP ameliorated the synovial IL-1β luciferase activity, reduced inflammatory cell infiltration and alleviated the erosive damage in the cartilage.

Conclusion: The anti-inflammatory properties of potassium channel inhibitors, especially of oATP, might point to new strategies for local anti-inflammatory therapy for acute gout.

Keywords: acute gout, interleukin-1β, potassium channel, local treatment

Introduction

Acute gouty arthritis is an inflammatory disease caused by precipitation of monosodium urate (MSU) crystals, which stimulate the production of interleukin-1β (IL-1β) and initiate an inflammatory reaction in the synovium and joint fluid.[1] Gouty arthritis is the most prevalent inflammatory arthritis in men and is associated with impaired quality of life.[2] MSU crystals lead to the onset of acute gouty arthritis mainly through the activation of Toll-like receptors (TLRs) and NACHT-LRR-PYD-containing protein 3 (NALP3) inflammasome signaling and the stimulation of IL-1β.[3] MSU crystals activate the NALP3 inflammasome by triggering an efflux of potassium ions into extracellular space, thereby reducing the concentration of cytoplasmic potassium.[4,5]

P2X7R, a ligand for purinergic receptor P2X ligand-gated ion channel 7, mediates a non-selective cation conductance when stimulated with extracellular ATP.[6,7] Related studies have suggested that the P2X7R signaling pathway might be involved in regulating IL-1β secretion during the development of acute gouty arthritis.[8,9] It is well known that extracellular ATP is an important danger signal that activates the NALP3 inflammasome.[10–12] The outflow of potassium, which is induced by the binding of extracellular ATP to P2X7R, can stimulate the NALP3 inflammasome and further IL-

Received: 16 May 2023
Accepted: 4 August 2023
Published: 22 August 2023

1β secretion.[13] The voltage-gated KCNQ1 (KvLQT1, Kv7.1) potassium channel is encoded by a gene newly identified in gout patients of Han Chinese descent by Li et al's genome-wide associated study (GWAS).[14] This gene has been demonstrated to be associated with susceptibility to type 2 diabetes[15,16] as well as cardiac function.[17,18] In mice, the loss of *KCNQ1* leads to alterations in the genes involved in innate immune responses.[19]

To understand whether potassium channel antagonists attenuate local inflammation of gout, we employed the *cHS4I-hIL-1βP-Luc* transgenic mice in which the expression of a luciferase reporter gene was under the control of human IL-1β gene promoter.[20] Luciferase gene expression was monitored in living mice under anesthesia using bioluminescence imaging in the synovium-like subcutaneous air pouch gouty arthritis model. This model enables us to non-invasively study the level of IL-1β gene expression in real time and to evaluate the effects of blockers on IL-1β gene induction in vivo. Here, to further investigate the role of P2X7R and KCNQ1 inhibitors in the process of acute gouty arthritis, we examined IL-1β gene expression pattern after subcutaneous injection of MSU alone and with each inhibitor into air pouches of mice. The dissection of this pathway for cytokine release may disclose new strategies for local anti-inflammatory therapy.

Methods

Preparation of MSU Crystal

Synthetic MSU crystals were prepared as follows. Briefly, a solution of 10mM uric acid (Sigma-Aldrich, St. Louis, MO) and 154mM NaCl in phosphate-buffered saline (PBS) was made and adjusted to pH 9.0. The solution was stirred slowly and continuously at 37°C. Three days later, crystals were harvested by decanting the supernatant. Polarized light microscopic examination confirmed that the crystals were needle-shaped and uniform in size (5~25 μm in length). After washed twice by absolute alcohol and once by acetone, the crystals were dried under sterile conditions and sterilized at 180°C for 2 hours to remove potentially contaminating lipopolysaccharide (LPS).[21]

Drugs and Reagents

D-Luciferin (sodium salt; Gold Biotechnology, St. Louis, MO) was stored at −20 °C. Reagents of tetraethylammonium chloride (TEA), adenosine 5′-triphosphate, periodate oxidized sodium salt (oATP), chromanol 293B and dexamethasone were purchased from Sigma-Aldrich (St. Louis, MO, USA).

Cell Culture

Human monocyte cell line, THP-1 (Cell bank of Chinese Academy of Sciences, China), was cultured in RPMI 1640 (Gibco), supplemented with 10% fetal bovine serum (FCS), 50 mM β-mercaptoethanol and penicillin and streptomycin (100 μg/mL). Cells were plated in 24-well plates at a density of 5×10^5 cells/well and treated with 500 nM phorbol 12-myristate 13-acetate (PMA). After 3 hours, the medium was replaced by fresh RPMI 1640 and the cells were incubated overnight (37 °C, 5% CO_2). The following morning, the medium was changed to Optimem (Gibco) and cells were treated with stepwise concentrations of MSU (0, 50 μg/mL, 100 μg/mL and 200 μg/mL) for 0, 2 hours, 6 hours and 24 hours. For intervention experiments, cells were administrated with MSU and/or indicated drugs.

Differentiated THP-1 cells were pelleted and lysed with a syringe on ice with the following quantitative real-time RT-PCR. Supernatants were harvested for enzyme-linked immunosorbent assay (ELISA).

Quantitative Real-Time RT-PCR

Total RNA was isolated from the cell line using trizol reagent (Roche Pharmaceuticals) and then reverse transcribed using a Fast Quant RT kit (Takara-Bio), followed by amplification using primers for *pro-IL-1β, P2x7r, Kcnq1* and *Kv1.3* under the condition: 95 °C for 10 min and 40 cycles of 95 °C for 15s, 58 °C for 20s and 68 °C for 20s. Primer sequences were shown as: forward-*pro-IL-1β* (5'- CTGTCCTGCGTGTTGAAAGA −3') and reverse-*pro-IL-1β* (5'- CTGGGC AGACTCAAATTCCA'); forward-*P2x7r* (5'- ACAATGTTGAGAAACGGACTCTGA −3') and reverse-*P2x7r* (5'- CCGGCTGTTGGTGGAATCCACATC −3'); forward-*Kcnq1* (5'- GACAAAGACAATGGGGTGACTCCT −3') and reverse-*Kcnq1* (5'- GTCATAGCCGTCGACAGAGAA −3'); forward-*Kv1.3* (5'- AGTATATGGTGATCGAAGAGG −3')

and reverse-*Kv1.3* (5'- AGTGAATATCTTCTTGATGTT −3'); forward-*actin* (5'- TGGCATTGCCGACAGGAT −3') and reverse-*actin* (5'- GGGCCGGACTCGTCATACT −3').

Elisa

The released IL-1β, IL-6 and TNF-α levels of THP-1 cell-free supernatant were quantified using a commercial ELISA kit (R&D Systems) followed by the instruction.

Animals

IL-1β luciferase mice were generated by incorporating the firefly luciferase gene driven by a 4.5-kb fragment of human IL-1β gene promoter (cHS4l-hIL-1β). Transgenic offspring were identified by PCR using the primers as follows: forward-luc (5'- GAGAGCTCCTGAGGCAGAGA −3') and reverse-luc (5'- GCCTTATGCAGTTGCTCTCC −3'), specific for luciferase gene. Transgenic male mice at the age of 12 weeks were employed for the experiments. The animals were maintained in a temperature-controlled room (22 °C), with humidity at 55% and on a 12 h light-dark cycle (lights on from 7 a.m. to 7 p.m.) under specific pathogen free (SPF) conditions. We also adhere to and include the ARRIVE checklist accordingly.

Synovium-Like Subcutaneous Air Pouches Model of Acute Gout

Subcutaneous pouches were generated by the injection of sterile, filtered air to create an accessible space that developed a synovium-like membrane within 7 days, as previously described.[22] Briefly, anesthetized 12-week-old cHS4I-hIL -1βP-Luc transgenic mice were injected with 5 mL of sterile air into the subcutaneous tissue of the back, followed by a second injection of 3 mL of sterile air into the pouch 3 days later. The sterile MSU crystals were resuspended in endotoxin-free PBS just before injection into air pouches models.

In vivo Bioluminescence Imaging and Luciferase Activity Assay

D-Luciferin was dissolved in PBS and injected intraperitoneally at a dose of 150 mg/ kg body weight before imaging. Mice were anesthetized with isoflurane/ oxygen and placed successionally in the IVIS Spectrum CT in vivo imaging system chamber (PerkinElmer, USA). Photons emitted from specific regions were quantified using a Living Image 4.3 (PerkinElmer, USA). For visualization, the luminescent image was overlaid on a photographic image. The signal intensity is represented by radiance (p/s/cm^2/sr) and encoded by pseudocolors on the luminescent image.

Mice were injected with 1 mL drugs and subgrouped into 1) control group (PBS, *s.c.*), 2) MSU group (3.0 mg/mL MSU crystals, *s.c.*), 3) MSU + dexamethasone group (3.0 mg/mL MSU with 10 mg/kg dexamethasone, *s.c.*), 4) MSU + TEA group (3.0 mg/mL MSU with 50 mg/kg TEA, *s.c.*), 5) MSU + oATP group (3.0 mg/mL MSU with 250 μM oATP, *s.c.*), 6) MSU + 293B group (3.0 mg/mL MSU with 50 mg/kg 293B, *s.c.*). The detection time points were 0, 2, 6, 24 and 48 hours.

Cell Counting

Mice were killed and pouch fluids were harvested after 6 hours of MSU or drug administration by injecting 5 mL PBS containing 5 mM EDTA. Cells infiltrating from the air pouch were counted manually using a hemocytometer. Smears of cells from the air pouches were prepared by centrifugation of either 50 μL of the pouch exudates or 10^5 of cells in cytofunnels (ThermoShandon, Pittsburgh, PA) in a Cytospin centrifuge (ThermoShandon) at 110g for 2 minutes.

Pathology

For histologic analysis of the air pouches, frozen sagittal sections of the air pouch tissues after 48 hours drug stimulation were fixed in 75% ethanol and then stained with hematoxylin for 2–5 minutes. Sections were washed 3 times with PBS and incubated in ammonium hydroxide for 30 seconds, and then incubated with acid alcohol (0.5% HCl in 70% ethanol) for 30 seconds. Sections were then washed 3 times again and stained with hematoxylin and eosin.

Data Analysis

All experimental statistical analyses were performed using GraphPad Prism version 8 (GraphPad). Statistical analysis of group differences was assessed by ANOVA. Data are presented as mean ± SEM. Differences with $P < 0.05$ were considered statistically significant.

Results

Cells and Crystals Verification

We used MSU crystal-stimulated THP-1 cells to detect inflammation and potassium channel changes. As shown in Figure 1A, the THP-1 cells were suspended with round surfaces. Three hours after PMA induction, the cells developed pseudopodia and became adherent (Figure 1B), making these cells suitable as a macrophage model. MSU crystals displayed birefringence under polarized light (Figure 1C). Six hours after MSU stimulation, crystals were engulfed by the THP-1 cells and traversed the whole cell (Figure 1D).

In vitro Effects of MSU Crystals on Inflammation

To determine the inflammation status of THP-1 cells, we collected cells with different concentrations of MSU (0, 50 μg/mL, 100 μg/mL and 200 μg/mL) after 6 hours. We employed the mRNA levels of *pro-Il-1β* as an indicator of the inflammation status. The results showed that the levels of *pro-Il-1β* increased with the escalation of MSU concentration (Figure 2A). The same results were observed in the mRNA levels of *P2x7r* (Figure 2B) and *Kv1.3* (Figure 2C). However, the mRNA levels of *Kcnq1*, a voltage-gated KCNQ channel, were decreased after MSU stimulation (Figure 2D).

Based on the data in Figures 2A–D, we selected 200 μg/mL MSU crystals as the most optimized concentration for in vitro stimulation. Time course of 0 hours, 2 hours, 6 hours and 24 hours with MSU intervention showed different levels of *pro-Il-1β* mRNA, which increased at the 2 hour time-point ($P < 0.05$), peaked at 6 hours ($P < 0.001$) and decreased after 24 hours ($P < 0.05$, Figure 2E). The same trends were detected in the mRNA levels of *P2x7r* (Figure 2F) and *Kv1.3* (Figure 2G). However, the mRNA levels of *Kcnq1* were down-regulated over time (Figure 2H).

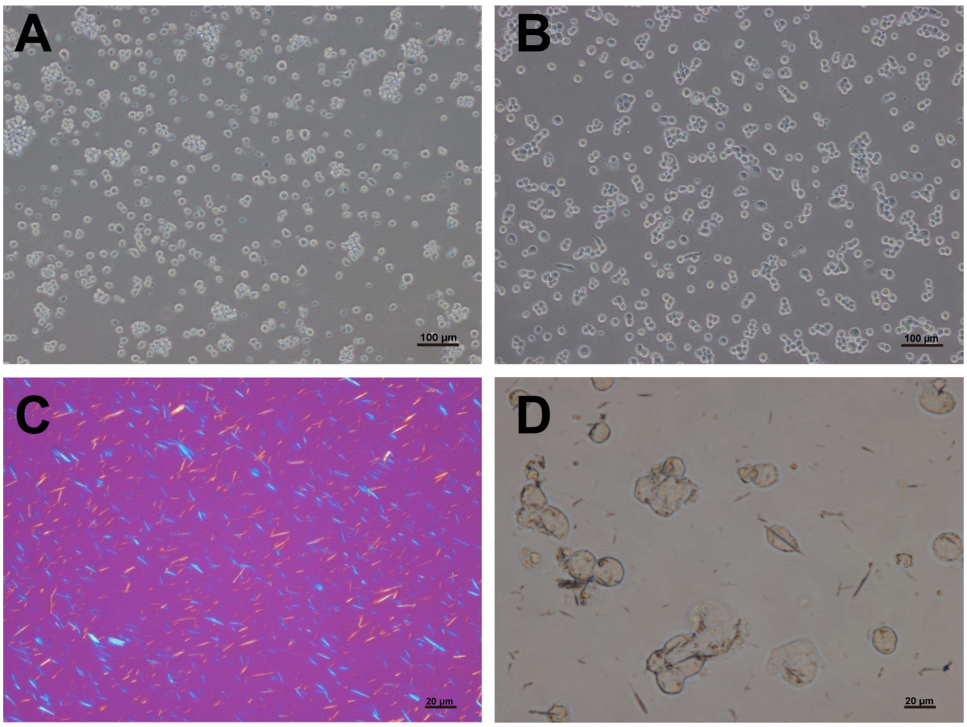

Figure 1 THP-1 cell morphology and phagocytosis of monosodium urate crystals. THP-1 cells were suspended with round surfaces (**A**) and then became adherent with pseudopodia after 3 hours of phorbol 12-myristate 13-acetate (PMA) induction (**B**). Monosodium urate (MSU) crystals showed birefringence under polarized light (**C**) and were engulfed by THP-1 cells (**D**). Bars = 20 μm or 100 μm as indicated. n=3/group.

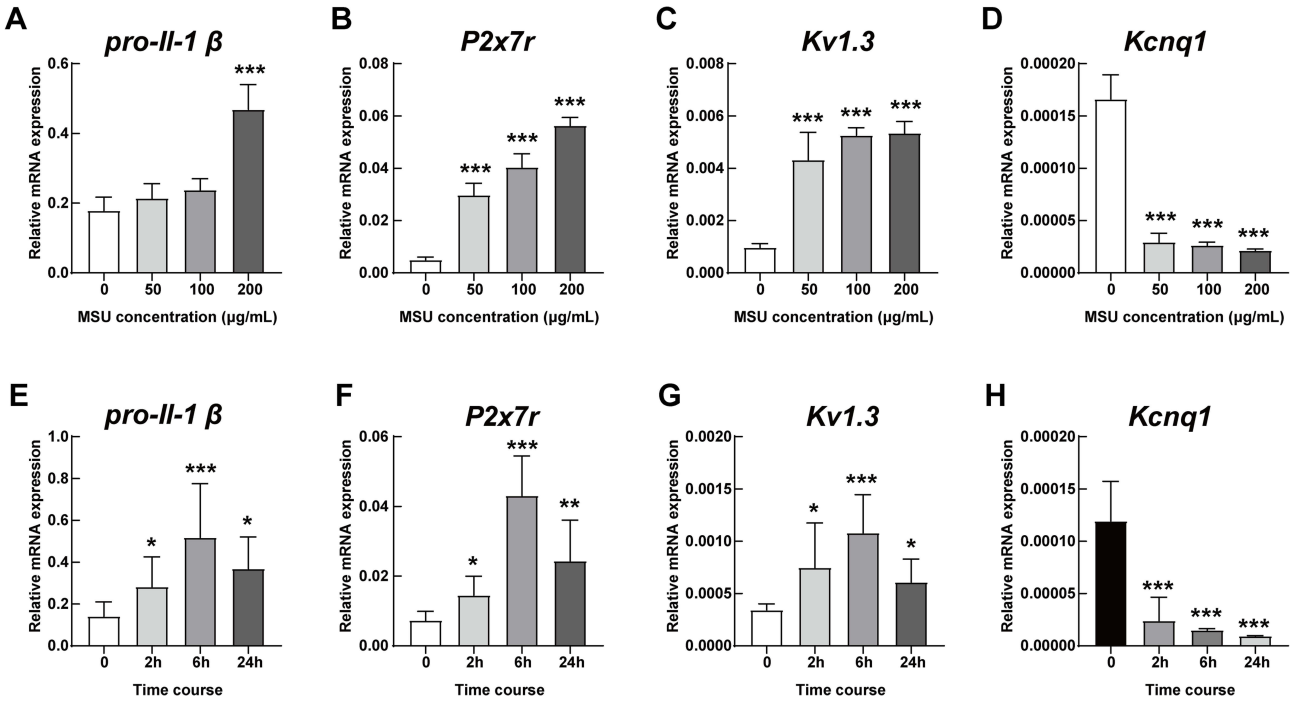

Figure 2 mRNA levels of potassium channels in a time- and concentration-dependent manner. The mRNA levels in THP-1 cells of (**A**) *pro-Il-1β*, (**B**) *P2x7r*, (**C**) *Kv1.3* and (**D**) *Kcnq1* under stepwise concentrations of MSU (0, 50 μg/mL, 100 μg/mL and 200 μg/mL) for 6 hours. The mRNA levels in THP-1 cells of (**E**) *pro-Il-1β*, (**F**) *P2x7r*, (**G**) *Kv1.3* and (**H**) *Kcnq1* treated with 200 μg/mL MSU for 0, 2 hours, 6 hours and 24 hours, respectively. *$P < 0.05$, **$P < 0.01$, ***$P < 0.001$, compared with the basal level. Data are expressed as mean ± SEM. n=3/group.

Effects of Potassium Channel Antagonists on Inflammation in vitro

Tetraethylammonium (TEA) is a non-selective potassium channel inhibitor, which inhibits ATP-sensitive (K_{ATP}) potassium channels in vitro and can also block the in vivo effects of K_{ATP} channel activators.[23] oATP is a potent, but unselective, P2X7R antagonist and can attenuate inflammatory responses independent of P2 receptor blockade.[24] We selected chromanol 293B as the potent specific KCNQ1 inhibitor.[25] When we used oATP and chromanol 293B, the levels of *P2x7r* and *Kcnq1* were inhibited accordingly (Figures 3A and B). Meanwhile, when TEA was administered to MSU-induced THP-1 cells, the levels of *P2x7r* mRNA expression were elevated (Figure 3A). The levels of secreted IL-1β, IL-6 and TNF-α in the supernatant were significantly up-regulated with MSU and dramatically down-regulated with high-dose potassium channel inhibitors, especially 900 μM oATP (Figure 3C–E). The levels of secreted IL-1β, IL-6 and TNF-α coincided with the mRNA levels of *P2x7r* and *Kcnq1* when stimulated with MSU (Figure 3).

Luciferase Activity in Acute Gouty Arthritis Mice

In the MSU-induced gouty arthritis model, a dramatic increase in luciferase activity was observed in the mice. The *cHS4l-hIL-1β* transgene induction was time-dependent and correlated with an increase in endogenous IL-1β mRNA levels. Inflammation following MSU injection into the subcutaneous air pouches of mice was detectable at 15 minutes, increased at 2 hours and 4 hours, peaked at 6 hours, and started to decline at 8 hours (Figure 4A). The inflammation was still detectable at 24 and 48 hours after the local treatment (Figure 4A).

As quantified by the Living Image software, this model showed a significant luciferase signal above the baseline level from 15 minutes to 48 hours after the MSU stimulation. At the peak, the luciferase signal was induced by 26.9-fold of the baseline level (Figure 4B).

In vivo Effects of Potassium Channel Antagonists on Inflammation

Based on the synovium-like subcutaneous air pouches model of acute gout, we exploited potassium channel blockers accompanied with 3.0 mg/mL MSU crystals. The 10 mg/kg dexamethasone group proxyed as a positive control, showing

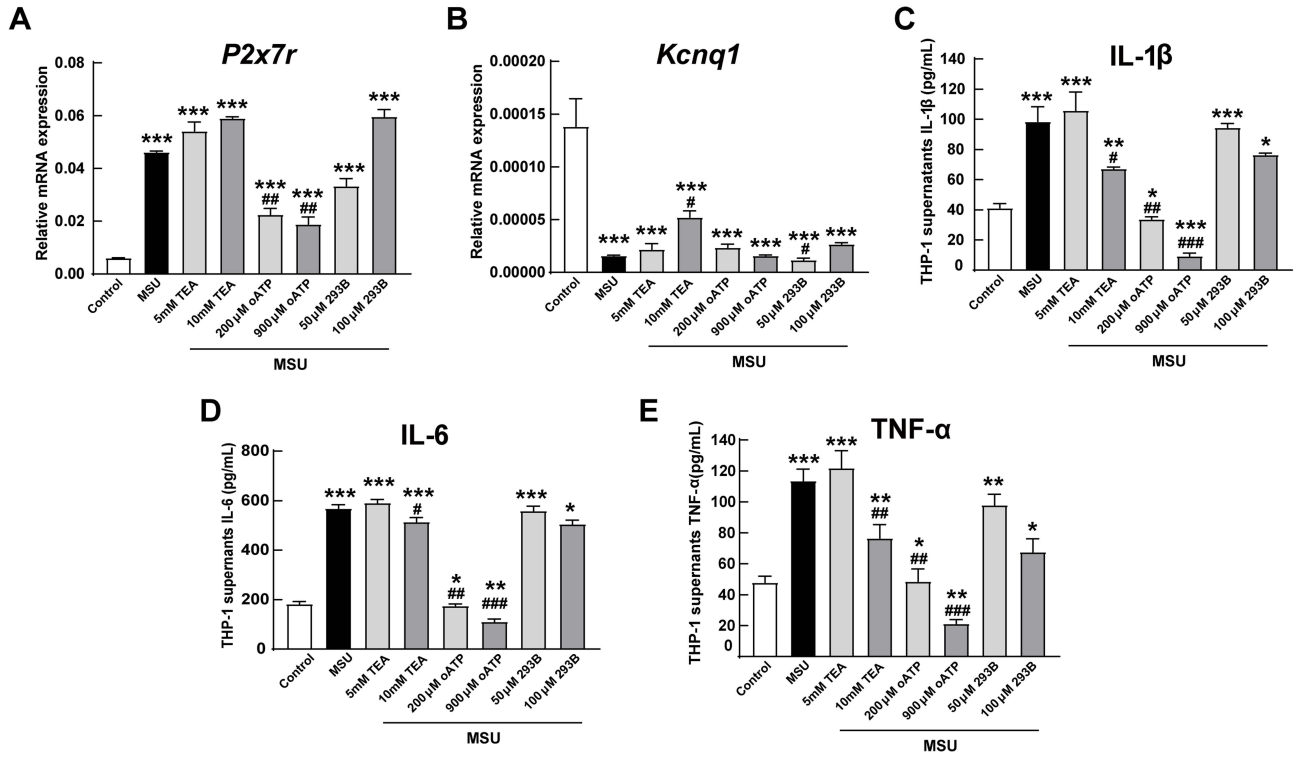

Figure 3 In vitro effects of potassium channel antagonists on inflammation. When treated with potassium channel antagonists tetraethylammonium chloride (TEA), adenosine 5′-triphosphate (ATP), periodate oxidized ATP (oATP) and chromanol 293B for 6 hours, the mRNA levels of *P2x7r* (**A**) and *Kcnq1* (**B**) in MSU-induced THP-1 cells were inhibited accordingly. The secreted levels of (**C**) IL-1β, (**D**) IL-6 and (**E**) TNF-α in supernatant with MSU and/or indicated antagonists. *$P < 0.05$, **$P < 0.01$, ***$P < 0.001$, compared with the control group. $^{\#}P < 0.05$, $^{\#\#}P < 0.01$, $^{\#\#\#}P < 0.001$, compared with the MSU group. Data are expressed as mean ± SEM. n=5 group.

a dramatic decrease in luciferase signal over time (Figure 5A). The TEA group had a weaker signal than the MSU group but stronger than the oATP group (Figure 5A). However, the 293B group had the highest luciferase signal (Figure 5A).

When we quantified the luciferase activity, the signal in all groups displayed a similar trend (Figure 5B). The signal increased from the 2nd hour, peaked at the 6th hour and declined by the 48th hour in all groups, except for the dexamethasone group, which peaked at the 2nd hour (Figure 5B). Significant differences were shown at the 6th hour among the groups (Figure 5C). The TEA group showed lower activities than the MSU group ($P < 0.05$, Figure 5C) but higher than the positive control ($P < 0.01$, Figure 5C). The oATP co-treated mice had 51.5% lower induced luciferase expression as compared with the MSU group ($P < 0.05$, Figure 5C). The luciferase activity was dramatically higher in the 239B group than that in the dexamethasone group ($P < 0.01$), but without a significant difference compared with the MSU group (Figure 5C).

Lavage Cell Counts and Air Pouch histopathology

At the sixth hour, the peak time of inflammation of the acute gout mice, we extracted their cells from the synovium-like subcutaneous air pouches. Similar to the luciferase activity data, the cell counting results showed a significant decrease in the dexamethasone group compared with the MSU group ($P < 0.001$, Figure 6A). Cell counts were also decreased in the oATP group ($P < 0.05$, Figure 6A), but TEA elevated the numbers of cells by 1.8-fold ($P < 0.05$, Figure 6A). The histological data showed a thickened synovium-like tissue locally with H&E staining at the 48th hour (Figure 6B). However, the synovium-like tissue thicknesses of the MSU + dexamethasone group and MSU + oATP group were thinner than those of the MSU group (Figure 6B).

Discussion

The role of MSU crystals in gout pathophysiology is well described, as is the major impact of IL-1β in the inflammatory reaction that constitutes the hallmark of the disease. However, despite the efflux of potassium stimulate the NALP3

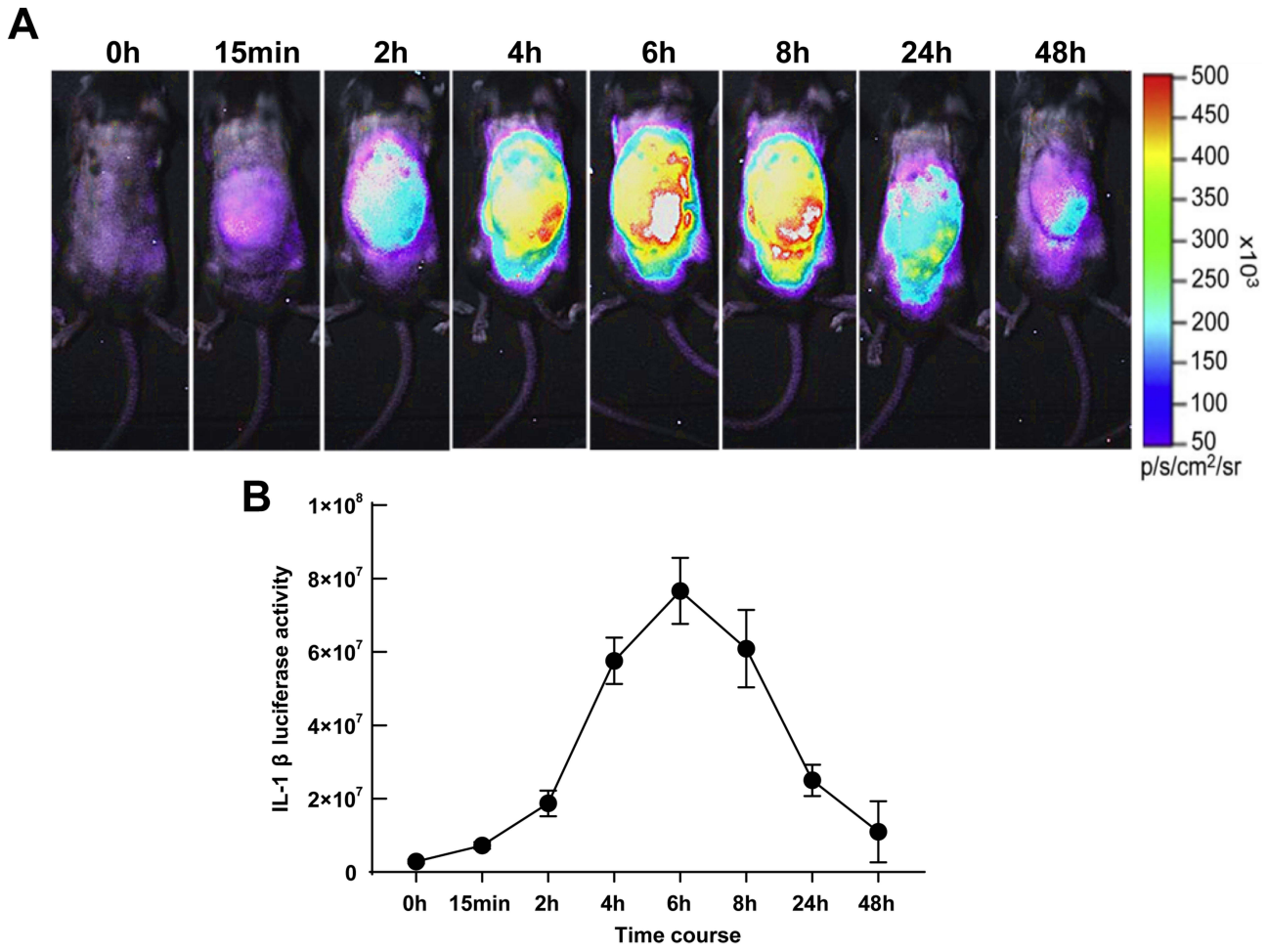

Figure 4 Luciferase activity in acute gouty arthritis mice. (**A**) The luciferase activities in MSU-induced *cHS4-hIL-1β* transgenic mice. (**B**) Quantitative measurements of IL-1β at 0, 15 minutes, 2 hours, 4 hours, 6 hours, 8 hours, 24 hours and 48 hours by the Living Image software as markers of inflammation status. n=5-7 mice/group.

inflammasome and further IL-1β secretion is well known, whether potassium inhibitor can relief inflammations and be used as a therapy regime are still poorly understood.

This is the first study to investigate the expression pattern of IL-1β in gouty arthritis model, using an in vivo bioluminescence imaging system. We reported that potassium channel inhibitors, especially oATP, alleviated MSU-induced gout inflammation as demonstrated by decreasing IL-1β levels in vitro and in vivo.

Release of IL-1β initiates and is a hallmark of acute gout flares. The export of caspase-1-processed IL-1β from macrophages has been proposed to be mediated by activation of P2X7, potassium efflux and the NLRP3 inflammasome assembly.[26] As shown in the genetic studies, single nucleotide polymorphisms (SNPs) of *P2X7R* were correlated to the susceptibility of primary gout in Chinese Han and Korean men.[27,28] Functionally, our study showed the P2X7R-potassium pathway mediates the inflammation of gout and gout flares could be released by P2X7R inhibitor.

The KCNQ1 is a voltage-gated potassium channel, forms a functional potassium selective pore and plays crucial roles in cardiac rhythm and extra-cardiac effects such as secretion of insulin.[29,30] The genetic mutations of *KCNQ1* gene have been reported to be related to type 2 diabetes,[31] cardiovascular diseases[32] and deafness.[33,34] Thus far, only a GWAS research of Han Chinese found a correlation of *KCNQ1* variants with gout while not hyperuricemia,[14] which mechanisms supposed be responsible of immune regulation. The amplification of inflammation of KCNQ1 blocker intervention in our gout mouse model was consistent with the hypothesis that KCNQ1 mediates gouty inflammation.

Additionally, Di et al[35] defined TWIK2 as an essential potassium efflux channel in macrophages and provided mechanistic insights into ATP-induced NLRP3 inflammasome activation and lung inflammation as when they inhibited

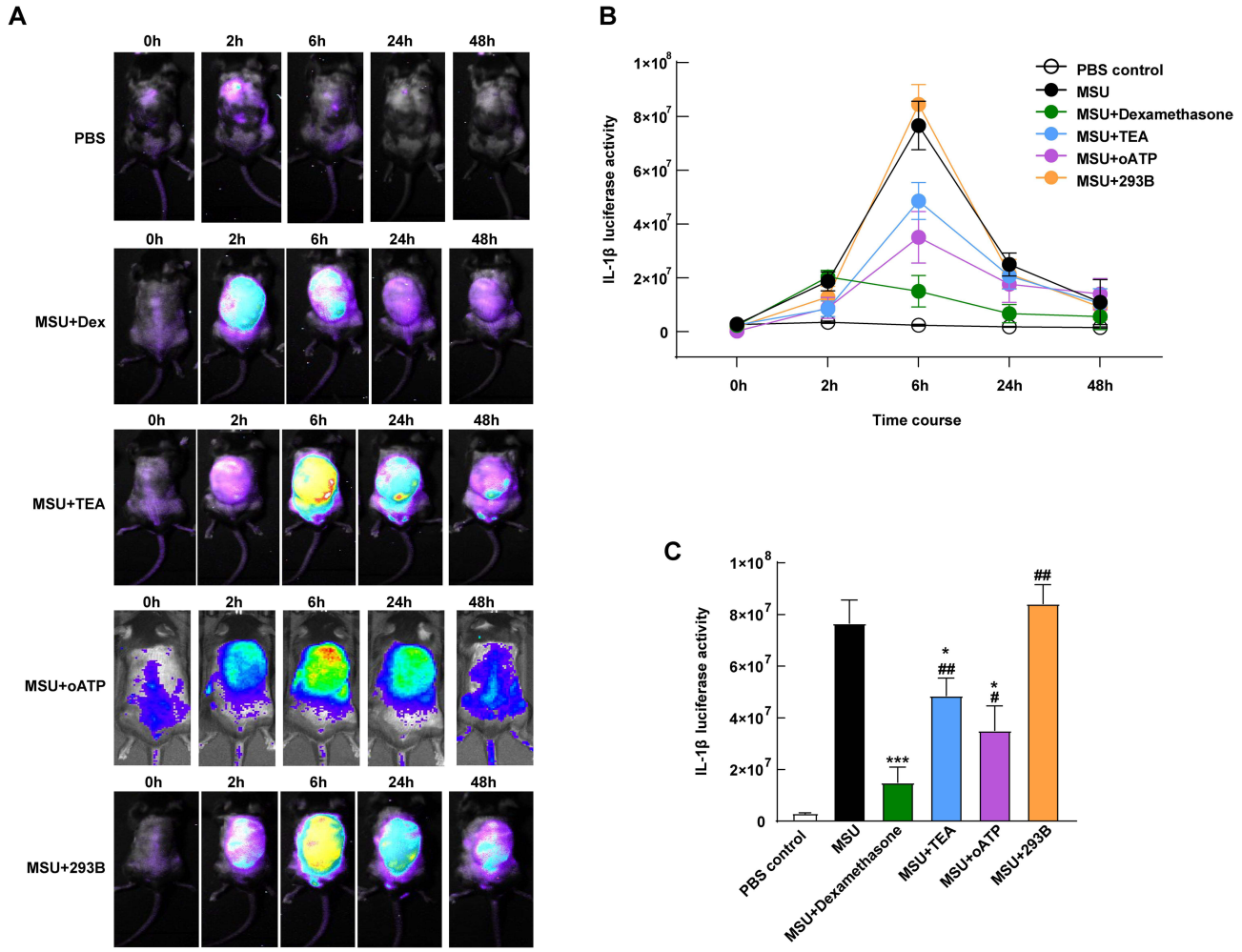

Figure 5 In vivo effects of potassium channel antagonists on inflammation. (**A**) The *cHS4-hIL-1β* transgenic mice were subgrouped into a control group (PBS, s.c.), MSU group (3.0 mg/mL MSU crystals, s.c.), MSU + dexamethasone group (3.0 mg/mL MSU with 10 mg/kg dexamethasone, s.c.), MSU + TEA group (3.0 mg/mL MSU with 50 mg/kg TEA, s.c.), MSU + oATP group (3.0 mg/mL MSU with 250 μM oATP, s.c.) and MSU + 293B group (3.0 mg/mL MSU with 50 mg/kg 293B, s.c.) Their luciferase activities were detected at 0, 2, 6, 24 and 48 hours. (**B**) The luciferase activities were quantified by the Living Image software and (**C**) compared at the sixth hour. $^{*}P < 0.05$, $^{***}P < 0.001$, compared with the control group. $^{\#}P < 0.05$, $^{\#\#}P < 0.01$, compared with the MSU group. Data are expressed as mean ± SEM. n=5-7 mice/group.

the TWIK2 in macrophages, the NLRP3 activation was prevented and sepsis-induced lung inflammation was suppressed. Though other potassium channels have been found to participant in the inflammation process, to inhibit most of the non-selective potassium channels by TEA could not maximize the effects of inflammation suppression in gout, as our results displayed.

Physiologically, potassium efflux plays its essential role in biological process. The principle of the administration of potassium channel blockers in vivo is to minimize the influences on normal physiological status. A local therapy has been a well-established way in arthropathies like osteoarthritis and rheumatoid arthritis.[36] In this study, we injected potassium channel inhibitors locally instead of systemically with a well response.

Conclusion

We developed a murine model of acute gout, with symptoms that consistent with the clinical symptoms of patients with acute gouty arthritis in the present study. Moreover, our study suggests that the inhibition of P2X7R channels alone or in combination with other treatments may provide an alternative choice for patients suffering acute attacks of gout who are less sensitive to or not tolerant of current medications.

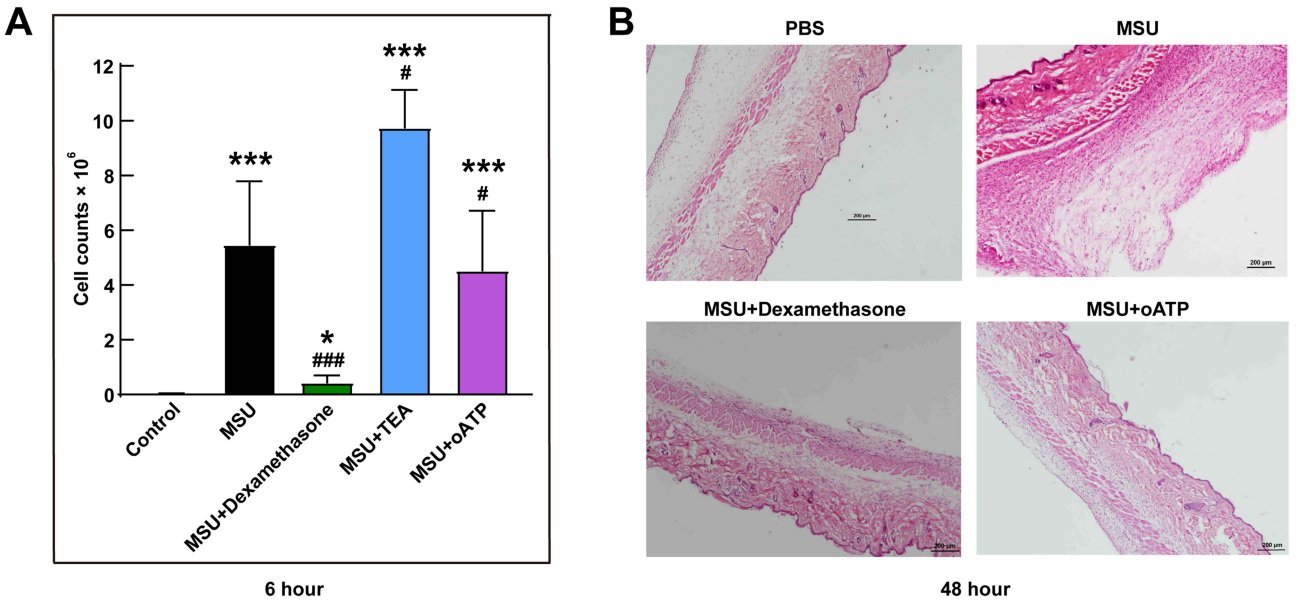

Figure 6 Lavage cell counts and air pouch histopathology. (**A**) Lavage cells were extracted from the synovium-like subcutaneous air pouches at the sixth hour and were manually counted using a hemocytometer. (**B**) The histology of synovium-like tissue stained by H&E staining after 48 hours stimuli. $^{*}P < 0.05$, $^{***}P < 0.001$, compared with the control group. $^{\#}P < 0.05$, $^{\#\#\#}P < 0.001$, compared with the MSU group. Data are expressed as mean ± SEM. n=5-7 mice/group.

Ethics Approval

All animal experiments were conducted in compliance with National Institutes of Health guidelines and were approved by the Animal Research Ethics Committee of the Affiliated Hospital of Qingdao University.

Acknowledgments

We really appreciate Prof. Changgui Li's team's support and help for our work, who are affiliated to the Shandong Provincial Clinical Research Center for Immune Diseases and Gout, Qingdao, China.

Author Contributions

All authors made a significant contribution to the work reported, whether that is in the conception, study design, execution, acquisition of data, analysis and interpretation, or in all these areas; took part in drafting, revising or critically reviewing the article; gave final approval of the version to be published; have agreed on the journal to which the article has been submitted; and agree to be accountable for all aspects of the work. All authors have read and approved the final submitted manuscript.

Funding

This work was sponsored by the Taishan Scholar Programme of Shandong Province (#tsqn202211377) and Shandong Provincial Science Foundation for Outstanding Youth Scholars (#ZR2021YQ56). No benefits in any form have been received or will be received from a commercial party related directly or indirectly to the subject of this article.

Disclosure

The authors report no conflicts of interest in this work.

References

1. Dalbeth N, Choi HK, Joosten LAB, et al. Gout. *Nat. Rev Dis Primers*. 2019;5(1):69. doi:10.1038/s41572-019-0115-y
2. Zhou W, Zhu J, Guo J, et al. Health-related quality of life assessed by Gout Impact Scale (GIS) in Chinese patients with gout. *Curr Med Res Opin*. 2020;36(12):2071–2078. doi:10.1080/03007995.2020.1840341
3. Shi Y, Mucsi AD, Ng G. Monosodium urate crystals in inflammation and immunity. *Immunol Rev*. 2010;233(1):203–217. doi:10.1111/j.0105-2896.2009.00851.x

4. Ferrari D, Pizzirani C, Adinolfi E, et al. The P2X7 receptor: a key player in IL-1 processing and release. *J Immunol*. 2006;176(7):3877–3883. doi:10.4049/jimmunol.176.7.3877
5. Petrilli V, Papin S, Dostert C, et al. Activation of the NALP3 inflammasome is triggered by low intracellular potassium concentration. *Cell Death Differ*. 2007;14(9):1583–1589. doi:10.1038/sj.cdd.4402195
6. Di Virgilio F, Dal Ben D, Sarti AC, et al. The P2X7 receptor in infection and inflammation. *Immunity*. 2017;47(1):15–31. doi:10.1016/j.immuni.2017.06.020
7. Dai X, Fang X, Xia Y, et al. ATP-activated P2X7R promote the attack of acute gouty arthritis in rats through activating NLRP3 inflammasome and inflammatory cytokine production. *J Inflamm Res*. 2022;15:1237–1248. doi:10.2147/JIR.S351660
8. Li X, Gao J, Tao J. Purinergic signaling in the regulation of gout flare and resolution. *Front Immunol*. 2021;12:785425. doi:10.3389/fimmu.2021.785425
9. Li X, Wan A, Liu Y, et al. P2X7R mediates the synergistic effect of ATP and MSU crystals to induce acute gouty arthritis. *Oxid Med Cell Longev*. 2023;2023:3317307. doi:10.1155/2023/3317307
10. Communi D, Janssens R, Suarez-Huerta N, et al. Advances in signalling by extracellular nucleotides. the role and transduction mechanisms of P2Y receptors. *Cell Signal*. 2000;12(6):351–360. doi:10.1016/S0898-6568(00)00083-8
11. Martinon F, Petrilli V, Mayor A, et al. Gout-associated uric acid crystals activate the NALP3 inflammasome. *Nature*. 2006;440(7081):237–241. doi:10.1038/nature04516
12. Tao JH, Zhang Y, Li XP. P2X7R: a potential key regulator of acute gouty arthritis. *Semin Arthritis Rheum*. 2013;43(3):376–380. doi:10.1016/j.semarthrit.2013.04.007
13. Jalilian I, Peranec M, Curtis BL, et al. Activation of the damage-associated molecular pattern receptor P2X7 induces interleukin-1beta release from canine monocytes. *Vet Immunol Immunopathol*. 2012;149(1–2):86–91. doi:10.1016/j.vetimm.2012.05.004
14. Li C, Li Z, Liu S, et al. Genome-wide association analysis identifies three new risk loci for gout arthritis in Han Chinese. *Nat Commun*. 2015;6:7041. doi:10.1038/ncomms8041
15. Xu J, Zhang W, Song W, et al. Relationship between KCNQ1 polymorphism and type 2 diabetes risk in northwestern China. *Pharmgenomics Pers Med*. 2021;14:1731–1751. doi:10.2147/PGPM.S340813
16. Yu XX, Liao MQ, Zeng YF, et al. Associations of KCNQ1 polymorphisms with the risk of type 2 diabetes mellitus: an updated meta-analysis with trial sequential analysis. *J Diabetes Res*. 2020;2020:7145139. doi:10.1155/2020/7145139
17. Chua HC, Servatius H, Asatryan B, et al. Unexplained cardiac arrest: a tale of conflicting interpretations of KCNQ1 genetic test results. *Clin Res Cardiol*. 2018;107(8):670–678. doi:10.1007/s00392-018-1233-3
18. Wang Z, Wang L, Liu W, et al. Pathogenic mechanism and gene correction for LQTS-causing double mutations in KCNQ1 using a pluripotent stem cell model. *Stem Cell Res*. 2019;38:101483. doi:10.1016/j.scr.2019.101483
19. Than BL, Goos JA, Sarver AL, et al. The role of KCNQ1 in mouse and human gastrointestinal cancers. *Oncogene*. 2014;33(29):3861–3868. doi:10.1038/onc.2013.350
20. Li L, Fei Z, Ren J, et al. Functional imaging of interleukin 1 beta expression in inflammatory process using bioluminescence imaging in transgenic mice. *BMC Immunol*. 2008;9:49. doi:10.1186/1471-2172-9-49
21. Schorn C, Frey B, Lauber K, et al. Sodium overload and water influx activate the NALP3 inflammasome. *J Biol Chem*. 2011;286(1):35–41. doi:10.1074/jbc.M110.139048
22. Yang Q, Zhang Q, Qing Y, et al. miR-155 is dispensable in monosodium urate-induced gouty inflammation in mice. *Arthritis Res Ther*. 2018;20(1):144. doi:10.1186/s13075-018-1550-y
23. Novakovic A, Pavlovic M, Milojevic P, et al. Different potassium channels are involved in relaxation of rat renal artery induced by P1075. *Basic Clin Pharmacol Toxicol*. 2012;111(1):24–30.
24. Koo TY, Lee JG, Yan JJ, et al. The P2X7 receptor antagonist, oxidized adenosine triphosphate, ameliorates renal ischemia-reperfusion injury by expansion of regulatory T cells. *Kidney Int*. 2017;92(2):415–431. doi:10.1016/j.kint.2017.01.031
25. Gao T, Li K, Liang F, et al. KCNQ1 potassium channel expressed in human sperm is involved in sperm motility, acrosome reaction, protein tyrosine phosphorylation, and ion homeostasis during capacitation. *Front Physiol*. 2021;12:761910. doi:10.3389/fphys.2021.761910
26. Ren W, Rubini P, Tang Y, et al. Inherent P2X7 Receptors Regulate Macrophage Functions during Inflammatory Diseases. *Int J Mol Sci*. 2021;23(1):232. doi:10.3390/ijms23010232
27. Lee SW, Lee SS, Oh DH, et al. Genetic Association for P2X7R rs3751142 and CARD8 rs2043211 polymorphisms for susceptibility of gout in Korean men: multi-center study. *J Korean Med Sci*. 2016;31(10):1566–1570. doi:10.3346/jkms.2016.31.10.1566
28. Ying Y, Chen Y, Li Z, et al. Investigation into the association between P2RX7 gene polymorphisms and susceptibility to primary gout and hyperuricemia in a Chinese Han male population. *Rheumatol Int*. 2017;37(4):571–578. doi:10.1007/s00296-017-3669-6
29. Huang H, Kuenze G, Smith JA, et al. Mechanisms of KCNQ1 channel dysfunction in long QT syndrome involving voltage sensor domain mutations. *Sci Adv*. 2018;4(3):eaar2631. doi:10.1126/sciadv.aar2631
30. van de Vondervoort I, Amiri H, Bruchhage MMK, et al. Converging evidence points towards a role of insulin signaling in regulating compulsive behavior. *Transl Psychiatry*. 2019;9(1):225. doi:10.1038/s41398-019-0559-6
31. Travers ME, Mackay DJ, Dekker Nitert M, et al. Insights into the molecular mechanism for type 2 diabetes susceptibility at the KCNQ1 locus from temporal changes in imprinting status in human islets. *Diabetes*. 2013;62(3):987–992. doi:10.2337/db12-0819
32. Tulay P, Temel SG, Ergoren MC. Investigation of KCNQ1 polymorphisms as biomarkers for cardiovascular diseases in the Turkish Cypriots for establishing preventative medical measures. *Int J Biol Macromol*. 2019;124:537–540. doi:10.1016/j.ijbiomac.2018.11.227
33. Torrado M, Fernandez G, Ganoza CA, et al. A cryptic splice-altering KCNQ1 variant in trans with R259L leading to Jervell and Lange-Nielsen syndrome. *NPJ Genomic Medicine*. 2021;6(1):21. doi:10.1038/s41525-021-00183-y
34. Homma K. The pathological mechanisms of hearing loss caused by KCNQ1 and KCNQ4 variants. *Biomedicines*. 2022;10(9):2254. doi:10.3390/biomedicines10092254
35. Di A, Xiong S, Ye Z, et al. The TWIK2 potassium efflux channel in macrophages mediates NLRP3 inflammasome-induced inflammation. *Immunity*. 2018;49(1):56–65 e4. doi:10.1016/j.immuni.2018.04.032
36. Wen J, Li H, Dai H, et al. Intra-articular nanoparticles based therapies for osteoarthritis and rheumatoid arthritis management. *Mater Today Bio*. 2023;19:100597. doi:10.1016/j.mtbio.2023.100597